

Arman B. Yeszhanov* , Ilya V. Korolkov , Maxim V. Zdorovets 

Institute of Nuclear Physics, Almaty, Kazakhstan
(*Corresponding author's e-mail: a.yeszhanov@inp.kz)

Graft Polymerization of Octadecyl Acrylate on PET Track-Etched Membranes for Direct Contact Membrane Distillation

Water purification is a critical environmental and social issue of our era. The contamination of water sources by industrial waste, agricultural chemicals, household debris, and plastic pollution significantly degrades the quality of available freshwater. This poses substantial threats to human health and ecosystems. While water is plentiful on Earth, only a limited amount is freshwater that people can safely consume. Population growth, urbanization, and climate change are further exacerbating this scarcity, especially in arid regions. This study examines the membrane distillation process employing ion-track membranes. Hydrophobic poly(ethylene terephthalate) ion-track membranes with increased pore diameters were synthesized via UV-induced graft polymerization of octadecyl acrylate on the membrane surface. Hydrophobic properties were assessed through water contact angle measurements. Fourier transform infrared spectroscopy analyzed functional groups while scanning electron microscopy examined surface morphology. The hydrophobic membranes were subsequently evaluated for desalination performance using direct contact membrane distillation method with saline solutions of varying concentrations. The effect of pore size and feed salt concentration on permeate flux and salt rejection efficiency was systematically examined. Membranes with a contact angle of $95\pm 3^\circ$ were tested in saline solutions with concentrations from 7.5 to 30 g/L.

Keywords: ion-track membranes, polymerization, membrane distillation, desalination, poly(ethylene terephthalate), salt rejection, water flux, water treatment

Introduction

The advancement of urbanization, together with rising population numbers and heightened industrial water usage, along with the escalating consequences of global climate change such as desertification and the reduction of freshwater sources may intensify the difficulties in maintaining dependable access to clean drinking water [1]. While approximately 70 % of the Earth's surface is covered by water, only about 2.5 % of it is fresh. Most of this fresh water is found in rivers, lakes, and groundwater. However, these resources are not always available or sufficient to meet the needs of the population [2, 3].

Industrial wastewater pollution is also one of the main threats to the environment and human health. Production processes in various industries are accompanied by the formation of significant amounts of waste that are discharged into water bodies. Without proper treatment, these effluents contain many toxic substances, which leads to the degradation of ecosystems, deterioration of water quality, and an increase in diseases. The shortage of fresh water resources and the problem of wastewater treatment highlight the urgent need to study innovative methods for the production of clean water on a large scale [4–9].

There is increasing focus on developing new, promising water purification methods that are more compact, cost-effective, and easier to operate than traditional techniques. Membrane separation processes, in particular, are gaining attention in the field of both natural and wastewater treatment [10–13]. Among the well-established methods, such as direct and reverse osmosis, as well as micro and ultrafiltration, the membrane distillation process is promising due to its energy efficiency, high degree of purification and flexibility in application. One of the main advantages of this process is its ability to operate at low temperatures, which makes it attractive for the use of low-potential or renewable energy sources. Membrane distillation does not require high pressure, which simplifies the design of the equipment and reduces operating costs [14–19].

In the membrane distillation (MD) process, the membrane plays a vital role as a selective barrier, preventing the passage of undesirable materials from the feed while allowing water vapor to pass through to the permeate side. MD membrane should meet specific requirements: high hydrophobicity and porosity, durability to sustain long-term operation.

Polymers predominantly utilized in the synthesis of membranes for membrane distillation (MD) applications include polytetrafluoroethylene (PTFE), polydimethylsiloxane (PDMS), polystyrene (PS), and poly(vinylidene fluoride) (PVDF). However, they have several disadvantages that can limit their performance and practicality for example thermal degradation, expensiveness of material, weak productivity. Therefore, the investigation of new types of membranes for MD is an urgent task [20–26].

One of the emerging types of membranes that have been successfully implemented in the MD process are ion-track membranes (TeMs) [27–32]. TeMs exhibit a range of advantageous physicochemical properties, including uniform pore morphology with controllable areal pore density, a narrowly dispersed pore size distribution characterized by low structural tortuosity, and reduced membrane thickness conducive to efficient mass transport. Currently, polymer matrices for the production of track-etched membranes are made from films of polycarbonate (PC), poly(ethyleneterephthalate) (PET), polyimide (PI), polypropylene and fluorinated polymers.

The use of PET TeMs in membrane distillation is appealing due to their unique properties. However, PET TeMs have low hydrophobic properties, which may limit their effective use in the MD process. Various surface modification methods are employed to improve hydrophobic properties. The simplest approaches to enhancing membrane hydrophobicity, such as graft polymerization, primarily involve depositing functional groups onto the membrane surface.

In our previous studies [27–32], PET TeMs were modified through ultraviolet (UV) initiated graft polymerization using different monomers and effectively applied in water desalination via membrane distillation. This study focuses on the fabrication of hydrophobic PET TeMs with large pore sizes by grafting octadecyl acrylate (OA) and their application in desalination processes.

Experimental

Chemical Substances

Hostaphan® brand PET film manufactured by Mitsubishi Polyester Film (Germany) with a nominal thickness of 12 μm was used. Sodium hydroxide (NaOH), benzophenone ($\text{C}_{13}\text{H}_{10}\text{O}$), N,N -dimethylformamide ($\text{C}_3\text{H}_7\text{NO}$), ethyl alcohol ($\text{C}_2\text{H}_5\text{OH}$), isoproryl alcohol ($\text{C}_3\text{H}_8\text{O}$), octadecyl acrylate ($\text{C}_{21}\text{H}_{40}\text{O}_2$, 97 %), sodium chloride (NaCl) were purchased from Sigma-Aldrich. Octadecyl acrylate was subjected to separation using a column packed with alumina. All experiments were conducted using deionized water with a resistivity of 18.2 $\text{M}\Omega\cdot\text{cm}$ at 25 $^\circ\text{C}$.

Photoinitiated Graft Polymerization of Octadecyl Acrylate

PET films samples (12 μm) were irradiated in a DC-60 (Astana branch of Institute of Nuclear Physics, Kazakhstan) heavy ion accelerator with a pore fluence of $1\cdot 10^6$ ion/ cm^2 . The chemical etching procedure was carried out according to the parameters established in previous studies [27–31].

The experimental procedure entailed the submersion of samples in a solution comprising octadecyl acrylate and isopropyl alcohol. The concentrations of the solution varied from 5 % to 30 %, with the incorporation of 0.0016 M benzophenone initiator. Dual-sided graft polymerization was performed under an OSRAM Ultra Vitalux E27 UV lamp (UVA: 315–400 nm, 13.6 W; UVB: 280–315 nm, 3.0 W), with distance from the UV lamp of 10 cm, with a total reaction time limited to 60 minutes. After the grafting process, the samples underwent washing, drying, and gravimetric analysis to quantify the grafting degree by the equation:

$$\omega = \frac{(m_2 - m_1)}{m_1} \cdot 100 \%, \quad (1)$$

where m_1 is the weight of the membrane before grafting, m_2 is the weight of the membrane after grafting.

Membrane Property Characterization Methods

InfraLUM FT-08 was used to analyze the functional groups present on the membrane surface. Data were recorded at 25 $^\circ\text{C}$. The Fourier transform infrared spectroscopy (FTIR) analysis was performed with a spectral resolution of 2 cm^{-1} , averaging 32 scans per sample, over a wavenumber range of 4000–400 cm^{-1} .

Hitachi TM 3030 scanning electron microscope was employed for the pore diameters evaluation.

The membrane pore size was also determined by the gas permeability method at a pressure of 20 kPa.

Quantitative assessment of the wetting properties of surfaces was carried out by measuring contact angles. The surface hydrophobicity was evaluated via static sessile drop method (on five random zones of sam-

ples) using Digital Microscope (Micron-400, China). The captured contact angle images were analyzed using the ImageJ software.

Testing of Hydrophobic PET TeMs in Membrane Distillation

Membrane distillation (MD) experiments were carried out using a DCMD setup, with the system specifications detailed in our earlier studies [32]. The membrane was installed in a specially designed experimental cell for conducting the membrane distillation (MD) process. The flow rates on both sides were regulated and sustained using a peristaltic pump. A consistent temperature difference of 70 ± 5 °C was maintained throughout the experiment. Permeate flux was calculated by weighing the amount of permeate collected. The experiments were conducted using saline solutions with varying NaCl concentrations. Salt rejection was determined using a HI2030-01 salinity meter.

The pure water permeation flux was calculated using the formula [32]:

$$Q = \frac{m}{S \cdot t}, \quad (2)$$

where Q is a pure water permeation flux ($\text{kg}/\text{m}^2 \cdot \text{h}$); m is an amount of permeate mass (kg); t is a time interval (hr); S is a membrane area (m^2).

The standard deviation (SD) was calculated using the formula:

$$s = \sqrt{\frac{1}{n-1} \sum_{i=1}^n (x_i - \bar{x})^2}, \quad (3)$$

where s is a standard deviation; n is a number of replicates; x_i is an individual measurement values, \bar{x} is an average value.

Results and Discussion

The modification outline of PET TeMs is presented in Figure 1. UV-photoinitiated graft polymerization is an efficient and environmentally friendly method for modifying polymer materials, which uses ultraviolet radiation to initiate the grafting of monomers onto the polymer surface. Figure 1a illustrates the UV-photoinitiated graft polymerization process, which begins with the activation of a photoinitiator. Upon absorption of UV light, the photoinitiator enters an excited state which, which leads to the formation of free radicals. Figure 1b shows the interaction of radicals with monomer molecules, initiating their polymerization and forming grafted polymer chains on the surface of the base material. Key features of this method include a high reaction rate at room temperature, no need for heating or high pressure, which prevents thermal degradation of the polymer and preserves its original physical and chemical properties. UV-induced graft polymerization is a resource-efficient technique characterized by low energy consumption and the absence of toxic solvent usage, making it an environmentally friendly method [33].

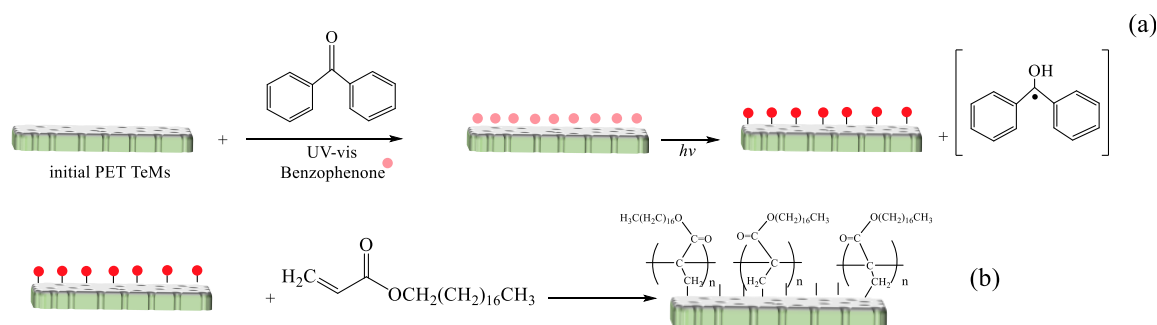


Figure 1. Scheme of UV-photoinitiated graft polymerization of octadecyl acrylate

Figure 2 shows the FTIR spectra for the identification of functional groups before and after modification with octadecyl acrylate. The characteristic absorption bands of unmodified PET TeMs have been previously reported [29–31]. Upon grafting with OA, new absorption peaks appeared at approximately ~ 2920 cm^{-1} and 2850 cm^{-1} , corresponding to the C–H stretching vibrations. The intensity of these peaks increases with increasing OA concentration.

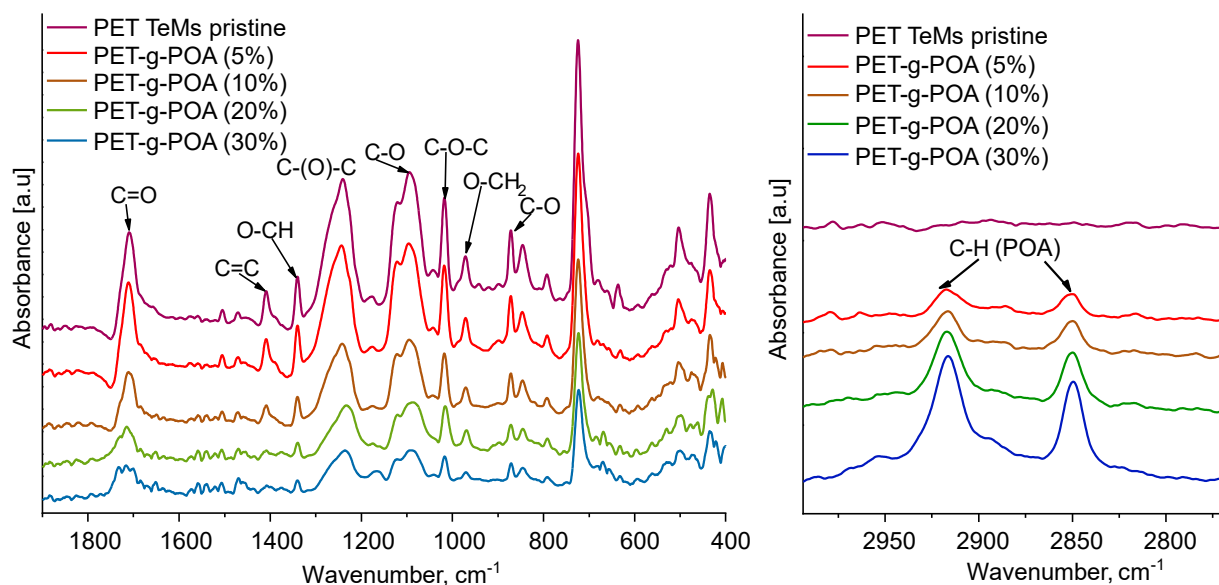


Figure 2. FTIR spectra comparison of pristine and poly(octadecyl acrylate)-grafted PET ion-track membranes over selected spectral ranges

Figure 3 demonstrates the effect of monomer concentration and irradiation time on the grafting degree. It was demonstrated that the optimal reaction condition is an OA concentration of 10 % (the degree of grafting is 3.39 %). However, it is also important to note that increasing the concentration of OA leads to changes in the morphology of the membrane surface, leading to pore overgrowth. Thus, at a concentration of octadecyl acrylate of 20 %, the grafting degree was 5.29 %, and at 30 % — 9.17 %. Figure 3b demonstrates that the grafting degree increases with irradiation time. The optimal duration for maintaining the pore structure is 60 minutes, while extending the irradiation time further results in surface degradation of the PET TeMs.

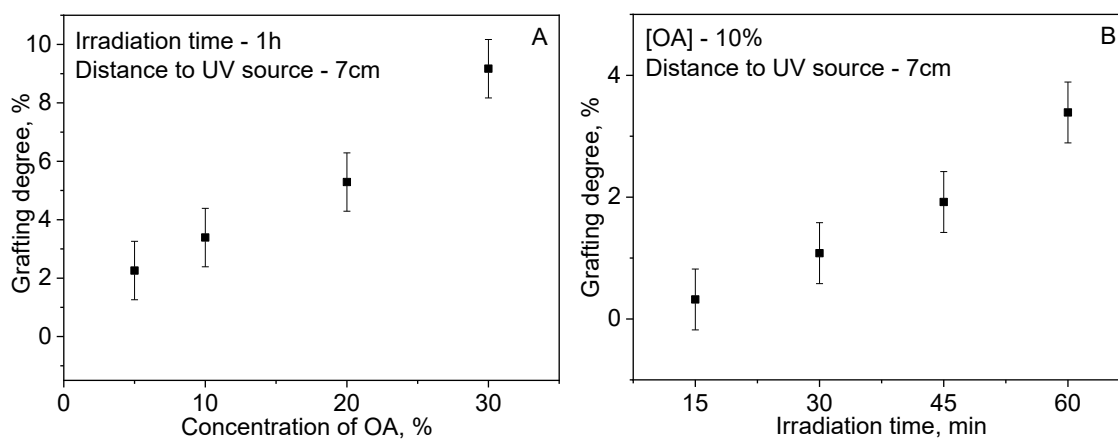


Figure 3. The effect of concentration OA and irradiation time on the grafting degree

The surface morphology of pristine and modified PET TeMs was analyzed using scanning electron microscopy (SEM). The results of the pore diameter values are presented in Table 1. SEM images of the initial and modified membranes are shown in Figure 4. SEM images demonstrate that increasing the concentration of octadecyl acrylate leads to a gradual decrease in the membrane pore size. Thus, at a concentration of 10 %, the pore size decreased from 920 ± 10 nm to 754 ± 8 nm with a grafting degree of 3.39 %.

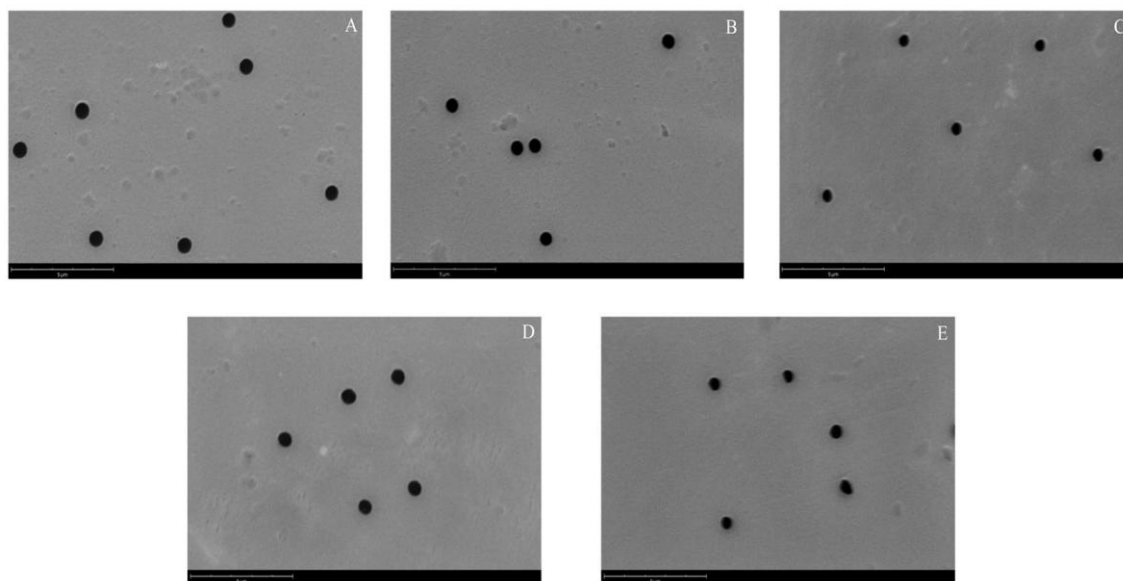


Figure 4. SEM images of pristine PET TeMs (a) and PET TeMs-g-POA (5 %) (b); (10 %) (c); (20 %) (d); 30 % (e)

Table 1

Characteristics of PET TeMs before and after OA modification

Sample	Concentration of OA, %	Graft yield, %	Effective pore size, nm	Pore size (SEM analysis), nm	Contact angle, °	Liquid Entry Pressure, MPa
PET TeMs	–	–	900±14	~920±10	~50-55	–
PET TeMs-g-POA	5	2.26	760±9	796±13	83°±3	0.15
	10	3.39	720±6	754±8	95°±3	≥0.34
	20	5.29	649±8	674±10	86°±4	≥0.39
	30	9.17	630±4	662±7	77°±2	≥0.5

Water contact angle (CA) measurements were employed to evaluate the hydrophobic properties. Figure 5 shows the CA values recorded at various locations on the PET TeMs before and after graft polymerization with octadecyl acrylate. The maximum contact angle is obtained at a 10 % concentration of octadecyl acrylate. A further increase in concentration reduces the value of the CA.

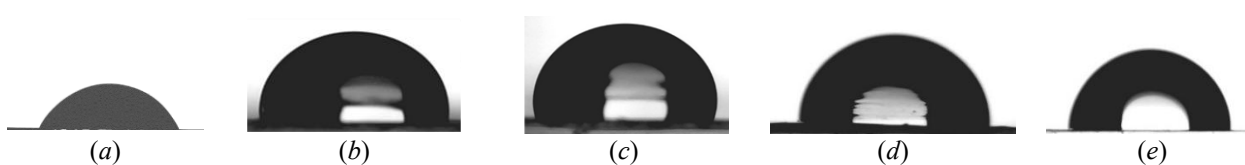


Figure 5. CA of the pristine PET TeMs (a), modified with OA (5 %) (b); (10 %) (c); (20 %) (d); 30 % (e)

Efficiency of Modified PET Ion-Track Membranes in Membrane Distillation Processes

Modified ion-track membranes (10 % of OA) pore sizes of 700 ± 25 nm and 980 ± 20 nm were evaluated in DCMD experiments using model saline solutions with NaCl concentrations of 7.5, 15, and 30 g/L. The experimental setup followed the procedure detailed in our previous publication [32]. The effect of membrane pore size and salt concentration on productivity and salt rejection was analyzed, with the corresponding results summarized in Table 2 and illustrated in Figure 6.

Table 2

Membrane distillation of saline solutions using PET TeMs-g-POA

	PET TeMs-g-POA with pore diameter of 725 nm	PET TeMs-g-POA with pore diameter of 1000 nm
NaCl 7.5 g/L	Degree of salt rejection — 96.16 % Water flow — 1.64 kg/m ² h	Degree of salt rejection — 81.37 % Water flow — 1.58 kg/m ² h
NaCl 15 g/L	Degree of salt rejection — 97.24 % Water flow — 1.42 kg/m ² h	Degree of salt rejection — 80.52 % Water flow — 1.28 kg/m ² h
NaCl 30 g/L	Degree of salt rejection — 96.12 % Water flow — 0.98 kg/m ² h	Degree of salt rejection — 70.38 % Water flow — 0.97 kg/m ² h

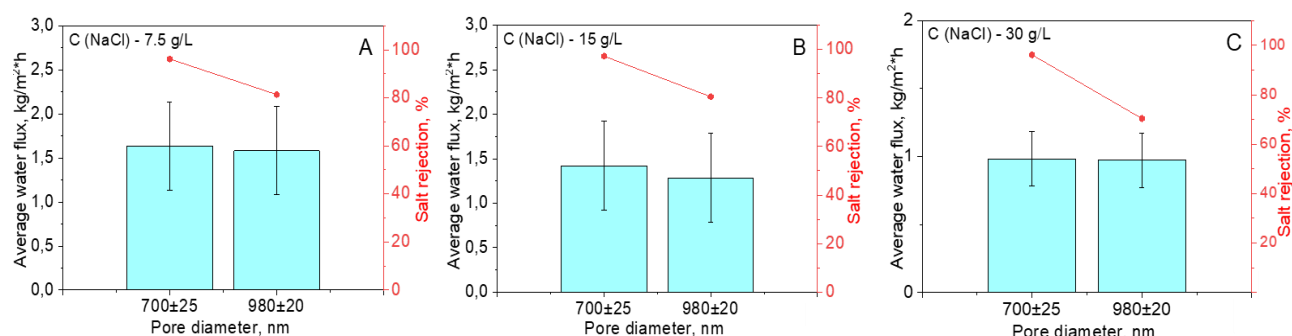


Figure 6. Productivity and salt rejection performance in DCMD experiments

Table 2 and Figure 6 illustrate the decreasing trend in water flux as the salt concentration increases, highlighting the adverse effect of salinity on membrane performance. Permeate flux of 1.64 ± 1 , 0.98 ± 1 was measured for membranes with pore diameters of 700 ± 25 nm using 7.5 and 30 g/L NaCl feed, respectively. In comparison, membranes with pore diameters of 980 ± 20 nm exhibited a water flux of $1.58 \text{ kg/m}^2\text{-h}$ at 7.5 g/L and $0.9713 \text{ kg/m}^2\text{-h}$ at 30 g/L, indicating a similar trend of decreasing productivity with increasing salt concentration. At a concentration of 15 g/L, the salt rejection rate was 97.24 % for membranes with 700 ± 25 nm pores and 80.52 % for those with 980 ± 20 nm pores.

Table 3 summarizes the characteristics and performance metrics of PET TeMs modified via various methods for application in MD.

Table 3

Relationship between pore size, LEP values and contact angle in PET TeMs modified by various methods, and their performance in membrane distillation process

Modification methods	Pore size, nm	Contact angle, °	Water flux, kg/m ² ·h	Salt rejection, %	LEP, MPa	Reference
UV-graft polymerization of TEVS and VIM	200 ± 18	105	0.088 — for 30 g/L NaCl	95.2	>0.430	[30]
UV-graft polymerization of styrene	220 ± 15	99	0.2193 — for 30 g/L NaCl	97.5	0.340	[31]
Immobilization of silica nanoparticles	263 ± 5	132	6.5 — for 30 g/L NaCl	98	0.430	[29]
UV-graft polymerization of lauryl methacrylate	724	94	1.88 — for 7.5 g/L NaCl	91.39	0.340	[32]
Electrospun PVDF nanofibers	300–5000	~140	4.68–6.78 —for 26.5 g/L NaCl	99.97	/	[34]
Electrospun PVC nanofibers	1159 ± 27 — 2494 ± 81	~155	13.61 — for 15 g/L NaCl	97.15	/	[35]

As can be seen in Table 3, surface modification by immobilization of silica nanoparticles resulted in the high degree of hydrophobization, achieving a contact angle of 132° and a water flux of $6.5 \text{ kg/m}^2\text{h}$ when treating a 30 g/L NaCl solution [29]. However, this method presents certain limitations, including high labor intensity and the gradual degradation of the nanoparticle layer during prolonged operation. One of the key challenges in membrane hydrophobization remains the development of methods capable of effectively treating membranes with large pore diameters, as these are directly correlated with higher productivity rates. Such modifications must maintain a high level of salt rejection to ensure the feasibility of MD processes under real-world conditions.

Among the studied approaches, hybrid membranes fabricated by electrospinning on the surface of TeMs poly(vinylidene fluoride) (PVDF) and poly(vinyl chloride) (PVC) nanofibers demonstrated outstanding performance in terms of both water flux and salt rejection. PVDF-based membranes showed water flux values ranging from 4.68 to $6.78 \text{ kg/m}^2\text{h}$ with nearly complete salt rejection (99.97%) for a 26.5 g/L NaCl solution [34], while PET TeMs-PVC nanofibers reached a flux of $13.61 \text{ kg/m}^2\text{h}$ and 97.15% salt rejection at 15 g/L NaCl concentration [35]. UV-induced graft polymerization of lauryl methacrylate (LMA) [32] enabling moderate hydrophobization (contact angle of 94°) and flux values of $1.88 \text{ kg/m}^2\text{h}$ with salt rejection above 91% for PET TeMs with $\sim 720 \text{ nm}$ pores.

In the present study, UV-initiated graft polymerization of octadecyl acrylate (OA) onto PET TeMs was carried out under optimized conditions ($10 \text{ wt}\%$ OA, UV exposure 60 min , 10 cm from UV lamp). This method provided effective hydrophobization of membranes with large pore diameters (725 and 1000 nm), achieving salt rejections of 96.16% and 81.37% , respectively, for a 7.5 g/L NaCl solution. Although hybrid PET TeMs demonstrate higher water flux in membrane distillation, their multilayered structure remains a critical disadvantage. Over time, this layered architecture may degrade. In contrast, the formation of covalent bonds during photoinitiated graft polymerization can overcome this disadvantage by ensuring strong interfacial adhesion between the functional layer and the membrane surface. Compared to lauryl methacrylate (LMA), octadecyl acrylate (OA) demonstrated superior salt rejection performance, particularly for PET TeMs with larger pore diameters. This enhancement can be attributed to the longer alkyl chain of OA, which forms a more densely packed and hydrophobic surface layer.

Conclusions

The present study successfully accomplished a chemical modification of PET TeMs by octadecyl acrylate (OA). Hydrophobic PET TeMs were obtained by photoinitiated graft polymerization with controlled variation of monomer concentration and irradiation duration to optimize surface functionalization. The combined application of FTIR spectroscopy, SEM analysis, and contact angle measurements allowed a thorough assessment of the samples chemical composition, surface structure, and wettability properties. Grafting of OA at optimal conditions (concentration of OA — 10% , time — 60 min , distance from UV-lamp 10 cm) led to an increase in the contact angle to 95° . In membrane distillation (MD) tests, these hydrophobic PET TeMs exhibited a productivity of $1.64 \text{ kg/m}^2\text{h}$ and a purification rate of 96.16% with a membrane pore diameter of 725 nm , while membranes with a pore diameter of 1000 nm at the same NaCl concentration (7.5 g/L) showed a lower productivity of $1.58 \text{ kg/m}^2 \text{ h}$ and a purification rate of 81.37% .

Funding

This study was supported by the Ministry of Science and Higher Education of the Republic of Kazakhstan under grant numbers BR28713053 and AP14869096.

Author Information*

*The authors' names are presented in the following order: First Name, Middle Name and Last Name

Arman Bakhytzhonovich Yezhanov (*corresponding author*) — Master of Chemical Sciences, Junior Scientific Researcher, Astana Branch, Institute of Nuclear Physics of the Republic of Kazakhstan, Abylai-khan street 2/1, 010000, Astana, Kazakhstan; e-mail: a.yezhanov@inp.kz; <https://orcid.org/0000-0002-1328-8678>

Ilya Vladimirovich Korolkov — PhD, Associated Professor, Senior Researcher, Astana branch, Institute of Nuclear Physics of the Republic of Kazakhstan, Abylai-khan street 2/1, 010000, Astana, Kazakhstan; e-mail: i.korolkov@inp.kz; <https://orcid.org/0000-0002-0766-2803>

Maxim Vladimirovich Zdorovets — Candidate of Physical and Mathematical Science, Professor, Director, Astana Branch, Institute of Nuclear Physics of the Republic of Kazakhstan, Abylai-khan street 2/1, 010000, Astana, Kazakhstan; e-mail: mzdorovets@inp.kz; <https://orcid.org/0000-0003-2992-1375>

Author Contributions

The manuscript was prepared with contributions from all authors, and all authors have approved the final version for submission. **CRedit: Arman Bakhytzhonovich Yeszhanov** — investigation, writing-original draft, data curation, visualization; **Ilya Vladimirovich Korolkov** — supervision, writing-review & editing, project administration; **Maxim Vladimirovich Zdorovets** — financial support acquisition, data management.

Conflicts of Interest

The authors declare that they have no financial or personal conflicts of interest that could have affected the results reported in this study.

References

- 1 Shalaby, S. M., Zayed, M. E., Hammad, F. A., Menesy, A. S., & Elbar, A. R. A. (2024). Recent advances in membrane distillation hybrids for energy-efficient process configurations: Technology categorization, operational parameters identification, and energy recovery strategies. *Process Safety and Environmental Protection*, *190*, 817–838. <https://doi.org/10.1016/J.PSEP.2024.07.098>
- 2 Wang, Y., Liu, X., Ge, J., Li, J., & Jin, Y. (2023). Distillation performance in a novel minichannel membrane distillation device. *Chemical Engineering Journal*, *462*, 142335. <https://doi.org/10.1016/J.CEJ.2023.142335>
- 3 Khalifa, A., Etman, A., El-Adawy, M., Alawad, S. M., & Nemitallah, M. A. (2025). Development of membrane distillation powered by engine exhaust for water desalination. *Applied Thermal Engineering*, *258*, 124839. <https://doi.org/10.1016/J.APPLTHERMALENG.2024.124839>
- 4 Khalifa, A., Kotb, M., & M. Alawad, S. (2025). Energy-efficient and cost-effective water desalination using membrane distillation with air-cooled dehumidifier bank. *Energy Conversion and Management: X*, *25*, 100844. <https://doi.org/10.1016/J.ECMX.2024.100844>
- 5 AlMehrz, M., Shaheen, A., Ghazal, A., Almarzooqi, N., Raza, A., Zhang, T., & AlMarzooqi, F. (2024). Photothermal ZrN composite membranes for solar-driven water distillation. *Journal of Environmental Chemical Engineering*, *12*(5), 113763. <https://doi.org/10.1016/J.JECE.2024.113763>
- 6 Shaikh, J. S., Aswalekar, U., Ismail, S., & Akhade, A. (2024). The potential of integrating solar-powered membrane distillation with a humidification–dehumidification system to recover potable water from textile wastewater. *Chemical Engineering and Processing — Process Intensification*, *205*, 110036. <https://doi.org/10.1016/J.CEP.2024.110036>
- 7 Tian, M., Yin, Y., Zhang, Y., & Han, L. (2025). Membrane distillation goes green: Advancements in green membrane preparation and renewable energy utilization. *Desalination*, *597*, 118344. <https://doi.org/10.1016/J.DESAL.2024.118344>
- 8 Zhang, N., Zhang, J., Gao, C., Yuan, S., & Wang, Z. (2025). Emerging advanced membranes for removal of volatile organic compounds during membrane distillation. *Desalination*, *597*, 118372. <https://doi.org/10.1016/J.DESAL.2024.118372>
- 9 Abejón, R., Romero, J., & Quijada-Maldonado, E. (2024). Potential of membrane distillation for water recovery and reuse in water stress scenarios: Perspective from a bibliometric analysis. *Desalination*, *591*, 117989. <https://doi.org/10.1016/J.DESAL.2024.117989>
- 10 Ahmadi, H., Ziapour, B. M., Ghaebi, H., & Nematollahzadeh, A. (2024). Optimization of vacuum membrane distillation and advanced design of compact solar water heaters with heat recovery. *Journal of Water Process Engineering*, *67*, 106212. <https://doi.org/10.1016/J.JWPE.2024.106212>
- 11 Park, H. J., Park, H., Kim, J., Lee, K., Naddeo, V., & Choo, K. H. (2024). Enhancing sustainability: Upcycled membrane distillation for water and nutrient recovery from anaerobic membrane bioreactor effluent. *Chemical Engineering Journal*, *498*, 155267. <https://doi.org/10.1016/J.CEJ.2024.155267>
- 12 Pawar, R., & Vidic, R. D. (2024). Impact of surfactants used in oil and gas extraction on produced water treatment by membrane distillation. *Desalination*, *586*, 117906. <https://doi.org/10.1016/J.DESAL.2024.117906>
- 13 Zhang, R., Chen, Y., Wang, H., Duan, X., & Ren, Y. (2024). A Janus membrane with silica nanoparticles interlayer for treating coal mine water via membrane distillation. *Separation and Purification Technology*, *350*, 127995. <https://doi.org/10.1016/J.SEPPUR.2024.127995>
- 14 Maliwan, T., & Hu, J. (2025). Release of microplastics from polymeric ultrafiltration membrane system for drinking water treatment under different operating conditions. *Water Research*, *274*, 123047. <https://doi.org/10.1016/J.WATRES.2024.123047>
- 15 Park, Y., Choi, Y., Choi, J., Ju, J., Kim, B., & Lee, S. (2020). Effect of vibration on fouling propensity of hollow fiber membranes in microfiltration and membrane distillation. *Desalination and Water Treatment*, *192*, 11–18. <https://doi.org/10.5004/DWT.2020.25151>

- 16 Ortega-Bravo, J. C., Guzman, C., Iturra, N., & Rubilar, M. (2023). Forward osmosis, reverse osmosis, and distillation membranes evaluation for ethanol extraction in osmotic and thermic equilibrium. *Journal of Membrane Science*, *669*, 121292. <https://doi.org/10.1016/J.MEMSCI.2022.121292>
- 17 Ali, A. S., & Bounahmidi, T. (2024). Coupling of photovoltaic thermal with hybrid forward osmosis-membrane distillation: Energy and water production dynamic analysis. *Journal of Water Process Engineering*, *64*, 105710. <https://doi.org/10.1016/J.JWPE.2024.105710>
- 18 Otávio Rosa e Silva, G., Rodrigues dos Santos, C., Souza Casella, G., Pinheiro Drumond, G., & Cristina Santos Amaral, M. (2025). Membrane fouling in integrated forward osmosis and membrane distillation systems — A review. *Separation and Purification Technology*, *356*, 129955. <https://doi.org/10.1016/J.SEPPUR.2024.129955>
- 19 Wang, L., Sun, X., Gao, F., Yang, Y., & Song, R. (2024). Solar membrane distillation: An emerging technology for reverse osmosis concentrated brine treatment. *Desalination*, *592*, 118124. <https://doi.org/10.1016/J.DESAL.2024.118124>
- 20 Li, X., García-Payo, M. C., Khayet, M., Wang, M., & Wang, X. (2017). Superhydrophobic polysulfone/polydimethylsiloxane electrospun nanofibrous membranes for water desalination by direct contact membrane distillation. *Journal of Membrane Science*, *542*, 308–319. <https://doi.org/10.1016/J.MEMSCI.2017.08.011>
- 21 Bahrami Eynolghasi, M., Mohammadi, T., & Tofighy, M. A. (2022). Fabrication of polystyrene (PS)/cyclohexanol-based carbon nanotubes (CNTs) mixed matrix membranes for vacuum membrane distillation application. *Journal of Environmental Chemical Engineering*, *10*(4), 108175. <https://doi.org/10.1016/J.JECE.2022.108175>
- 22 Omar, N. M. A., Othman, M. H. D., Tai, Z. S., Kurniawan, T. A., Puteh, M. H., Jaafar, J., Rahman, M. A., Bakar, S. A., & Abdullah, H. (2024). A review of superhydrophobic and omniphobic membranes as innovative solutions for enhancing water desalination performance through membrane distillation. *Surfaces and Interfaces*, *46*, 104035. <https://doi.org/10.1016/J.SURFIN.2024.104035>
- 23 Jilagam, N. K., Vaghela, G., Chakrabarty, T., Guo, J., Farid, M. U., Jeong, S., Shon, H. K., An, A. K., & Deka, B. J. (2024). Frontier of metal-organic framework nanofillers for pre-eminent membrane distillation applications. *Desalination*, *592*, 118127. <https://doi.org/10.1016/J.DESAL.2024.118127>
- 24 Nthunya, L. N., Chong, K. C., Lai, S. O., Lau, W. J., López-Maldonado, E. A., Camacho, L. M., Shirazi, M. M. A., Ali, A., Mamba, B. B., Osial, M., Pietrzyk-Thel, P., Pregowska, A., & Mahlangu, O. T. (2024). Progress in membrane distillation processes for dye wastewater treatment: A review. *Chemosphere*, *360*, 142347. <https://doi.org/10.1016/J.CHEMOSPHERE.2024.142347>
- 25 Jawed, A. S., Nassar, L., Hegab, H. M., van der Merwe, R., Al Marzooqi, F., Banat, F., & Hasan, S. W. (2024). Recent developments in solar-powered membrane distillation for sustainable desalination. *Heliyon*, *10*(11), e31656. <https://doi.org/10.1016/J.HELIYON.2024.E31656>
- 26 Guo, Q., Liu, Y., Li, T., Gao, L., Yin, S., Li, S., & Zhang, L. (2024). Enhancement and optimization of membrane distillation processes: A systematic review of influential mechanisms, optimization and applications. *Desalination*, *586*, 117862. <https://doi.org/10.1016/J.DESAL.2024.117862>
- 27 Shakayeva, A. K., Yeszhanov, A. B., Borissenko, A. N., Kassymzhanov, M. T., Zhumazhanova, A. T., Khlebnikov, N. A., Nurkassimov, A. K., Zdorovets, M. V., Güven, O., & Korolkov, I. V. (2024). Surface Modification of Polyethylene Terephthalate Track-Etched Membranes by 2,2,3,3,4,4,5,5,6,6,7,7-Dodecafluoroheptyl Acrylate for Application in Water Desalination by Direct Contact Membrane Distillation. *Membranes*, *14*(7). <https://doi.org/10.3390/membranes14070145>
- 28 Yeszhanov, A. B., Korolkov, I. V., Dosmagambetova, S. S., Zdorovets, M. V., & Güven, O. (2021). Recent Progress in the Membrane Distillation and Impact of Track-Etched Membranes. *Polymers*, *13*(15). <https://doi.org/10.3390/polym13152520>
- 29 Korolkov, I. V., Kuandykova, A., Yeszhanov, A. B., Güven, O., Gorin, Y. G., & Zdorovets, M. V. (2020). Modification of PET Ion-Track Membranes by Silica Nanoparticles for Direct Contact Membrane Distillation of Salt Solutions. *Membranes*, *10*(11), 1–15. <https://doi.org/10.3390/MEMBRANES10110322>
- 30 Korolkov, I. V., Gorin, Y. G., Yeszhanov, A. B., Kozlovskiy, A. L., & Zdorovets, M. V. (2018). Preparation of PET track-etched membranes for membrane distillation by photo-induced graft polymerization. *Materials Chemistry and Physics*, *205*, 55–63. <https://doi.org/10.1016/J.MATCHEMPHYS.2017.11.006>
- 31 Korolkov, I. V., Yeszhanov, A. B., Zdorovets, M. V., Gorin, Y. G., Güven, O., Dosmagambetova, S. S., Khlebnikov, N. A., Serkov, K. V., Krasnopyorova, M. V., Milts, O. S., & Zheltov, D. A. (2019). Modification of PET ion track membranes for membrane distillation of low-level liquid radioactive wastes and salt solutions. *Separation and Purification Technology*, *227*, 115694. <https://doi.org/10.1016/J.SEPPUR.2019.115694>
- 32 Yeszhanov, A. B., Korolkov, I. V., Güven, O., Melnikova, G. B., Dosmagambetova, S. S., Borissenko, A. N., Nurkassimov, A. K., Kassymzhanov, M. T., & Zdorovets, M. V. (2024). Effect of hydrophobized PET TeMs membrane pore-size on saline water treatment by direct contact membrane distillation. *RSC Advances*, *14*(6), 4034–4042. <https://doi.org/10.1039/D3RA07475G>
- 33 Deng, J., Wang, L., Liu, L., & Yang, W. (2009). Developments and new applications of UV-induced surface graft polymerizations. *Progress in Polymer Science*, *34*(2), 156–193. <https://doi.org/10.1016/J.PROGPOLYMSCI.2008.06.002>
- 34 Kravets, L., Vinogradov, I., Rossouw, A., Gorberg, B., Nechaev, A., & Apel, P. (2025). Functionalization of PET track-etched membranes with electrospun PVDF nanofibers for hybrid membranes fabrication in water desalination. *Separation and Purification Technology*, *371*(March), 133395. <https://doi.org/10.1016/j.seppur.2025.133395>
- 35 Yeszhanov, A. B., Shakayeva, A. Kh., Zdorovets, M. V., Borgekov, D. B., Kozlovskiy, A. L., Kharkin, P. V., Zheltov, D. A., Krasnopyorova, M. V., Güven, O., & Korolkov, I. V. (2025). Hybrid Membranes Based on Track-Etched Membranes and Nanofiber Layer for Water–Oil Separation and Membrane Distillation of Low-Level Liquid Radioactive Wastes and Salt Solutions. *Membranes*, *15*(7), 202. <https://doi.org/10.3390/membranes15070202>